Science of the Total Environment 609 (2017) 764–775

Contents lists available at ScienceDirect

Science of the Total Environment

journal homepage: www.elsevier.com/locate/scitotenv

Performance assessment of individual and ensemble data-mining techniques for gully erosion modeling

Hamid Reza Pourghasemi [a], Saleh Yousefi [b], Aiding Kornejady [c], Artemi Cerdà [d,*]

[a] Department of Natural Resources and Environmental Engineering, College of Agriculture, Shiraz University, Shiraz, Iran
[b] Department of Watershed Management Engineering, Faculty of Natural Resources, Tarbiat Modares University, Iran
[c] Department of Watershed Management Engineering, Gorgan University of Agricultural Sciences and Natural Resources, Gorgan, Iran
[d] Soil Erosion and Degradation Research Group, Departament de Geografia, Universitat de València, Blasco Ibàñez 28, 46010 Valencia Spain

HIGHLIGHTS

- Gully erosion susceptibility mapping models were evaluated.
- The ME model showed 45% of the study area as highly susceptible to gullying.
- ANN-SVM model shown 34% of the study area as highly susceptible.
- The role of ensemble modeling in relevant to building accurate and generalized models.
- Results prepare an outline for further biophysical designs on gullies scatter.

GRAPHICAL ABSTRACT

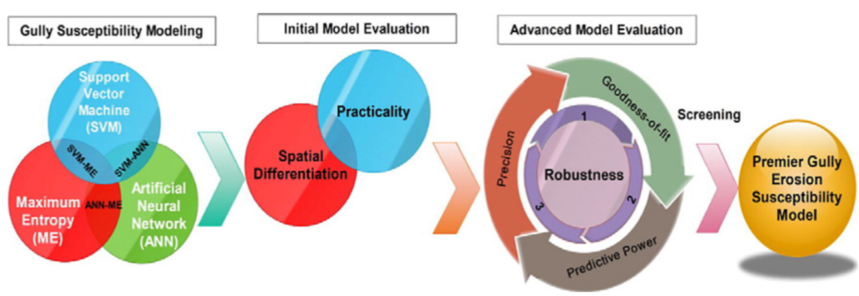

ARTICLE INFO

Article history:
Received 19 June 2017
Received in revised form 22 July 2017
Accepted 22 July 2017
Available online 29 July 2017

Editor: D. Barcelo

Keywords:
MaxEnt
SVM
ANN
Goodness-of-fit
Prediction power
Robustness
Vulnerability

ABSTRACT

Gully erosion is identified as an important sediment source in a range of environments and plays a conclusive role in redistribution of eroded soils on a slope. Hence, addressing spatial occurrence pattern of this phenomenon is very important. Different ensemble models and their single counterparts, mostly data mining methods, have been used for gully erosion susceptibility mapping; however, their calibration and validation procedures need to be thoroughly addressed. The current study presents a series of individual and ensemble data mining methods including artificial neural network (ANN), support vector machine (SVM), maximum entropy (ME), ANN-SVM, ANN-ME, and SVM-ME to map gully erosion susceptibility in Aghemam watershed, Iran. To this aim, a gully inventory map along with sixteen gully conditioning factors was used. A 70:30% randomly partitioned sets were used to assess goodness-of-fit and prediction power of the models. The robustness, as the stability of models' performance in response to changes in the dataset, was assessed through three training/test replicates. As a result, conducted preliminary statistical tests showed that ANN has the highest concordance and spatial differentiation with a chi-square value of 36,656 at 95% confidence level, while the ME appeared to have the lowest concordance (1772). The ME model showed an impractical result where 45% of the study area was introduced as highly susceptible to gullying, in contrast, ANN-SVM indicated a practical result with focusing only on 34% of the study area. Through all three replicates, the ANN-SVM ensemble showed the highest goodness-of-fit and predictive power with a respective values of 0.897 (area under the success rate curve) and 0.879 (area under the prediction rate curve), on average, and correspondingly the highest robustness. This attests the important role of ensemble modeling in congruently building accurate and generalized models which emphasizes the necessity to examine different models integrations. The result of this study can prepare an outline for further biophysical designs on gullies scattered in the study area.

* Corresponding author.
E-mail addresses: hr.pourghasemi@shirazu.ac.ir (H.R. Pourghasemi), artemio.cerda@uv.es (A. Cerdà).

http://dx.doi.org/10.1016/j.scitotenv.2017.07.198

1. Introduction

Water erosion is an integral part of geological and geomorphological cycle of the earth system. It also causes massive damages to agricultural lands and sometimes has irrecoverable and destructive impacts on dams, reservoirs, and water quality in semi-humid and arid areas (Mekonnen et al., 2017; Comino et al., 2016; Kheir et al., 2007; Buttafuoco et al., 2012). Amplified soil erosion rates have recently been related to the so called "environmental land use conflicts" (Pacheco et al., 2014; Valle Junior et al., 2014), which bear on uses of the land that deviate from its capability (natural use), and that these higher erosion rates tend to reduce soil fertility by important reductions in organic matter content (Valera et al., 2016). Gully erosion is a morphologically emerged process (Maslov, 2005) formed by water erosion with a substantial flow rate in a determined area. Generally, it causes deep cuts with tens of meters in depth and width which is imperceptibly initiated on a hillside and scours soil (Billi and Dramis, 2003). Gullies dramatically decrease soil productivity by incising agricultural lands and consequently cause restrictions in land use, roads, fences, and structures (Takken et al., 2008; Akgün and Türk, 2011; Mekonnen et al., 2017; Zakerinejad and Märker, 2015). As the most prominent feature, gullies remove upland soils along drainage lines by surface runoff and make it hard to conduct tillage operations (USDA-SCS, 1966). They are one of the most dominant causes of geo-environmental degradation in the west (Rahmati et al., 2016a) and the north part of the Iran due to present land uses and geoclimatic agents.

From data availability view point, data mining and statistical methods have been indisputably coped with data scarcity issue, especially those geophysical and geochemical data that are being used by the gully physical models such as CREAMS (Chemicals, Runoff, and Erosion from Agricultural Management Systems), EGEM (Ephemeral Gully Erosion Mode), and WEPP (Water Erosion Prediction Project) (Knisel, 1980; Flanagan and Nearing, 1995; Woodward, 1999). As noted by Conoscenti et al. (2013), these physical methods need to be tested before being used. Moreover, they do not assess gully erosion susceptibility, while susceptibility maps are the most important level of conceiving the exposition of an area to gullying. Different data mining, bivariate, and multivariate statistical methods have been used in many environmental fields. Some of these have been used for assessing gully erosion susceptibility including classification and regression trees (CART) (Gómez-Gutiérrez et al., 2009a, b; Märker et al., 2011), logistic regression (LR) (Chaplot et al., 2005a, b; Lucà et al., 2011; Conoscenti et al., 2014; Kornejady et al., 2015), information value (Conforti et al., 2011); weights of evidence (WofE) (Dube et al., 2014); frequency ratio (FR) (Rahmati et al., 2016a); multivariate adaptive regression splines (MARS) (Gómez-Gutiérrez et al., 2015), and random forest (RF) (Kuhnert et al., 2010). Thus, a wide range of data mining methods has still remained unused. For instance, maximum entropy model has been widely employed in different fields such as environmental and ecological science (Phillips et al., 2004; Phillips and Dudík, 2008; Fourcade et al., 2014; Ariyanto, 2015; Cao et al., 2016) and landslide susceptibility mapping (Kim et al., 2015; Davis and Blesius, 2015; Dickson and Perry, 2016; Kornejady et al., 2017). The support vector machine (SVM) and artificial neural network (ANN) also were applied in landslide field (Tsangaratos and Benardos, 2014; Ren et al., 2015; Tien Bui et al., 2016; Chen et al., 2017). On the other hand, ensemble modeling is getting more popular nowadays due to their accurate results. It can integrate models to achieve high performance results in terms of goodness-of-fit and predictive power in an efficient amount of time (Moonjun, 2007; Nefeslioglu et al., 2010; Pradhan, 2013; Umar et al., 2014). This being a tangible gap in gully erosion assessments, the objectives of this work are the following: 1) Use of three individual models (ANN, SVM, ME) and their ensembles (ANN-SVM, ANN-ME, and SVM-ME) in Aghemam Watershed; 2) conducting initial performance assessment statistics; 3) Calibrating the models by assessing the goodness-of-fit; and 4) validating the results by assessing the predictive power, precision, and robustness.

2. Material and methods

2.1. Study area

The Aghemam Watershed has an area of 2595 ha and is situated in the east of Golestan Province in northern Iran (Fig. 1), with an altitude range between 357 and 822 m asl. Average slope of study watershed is about 13% and the maximum length is 9.4 km. The main channel length in the study area is about 10.4 km with an average slope of 4%. Silty-loamy (about 87.5%) and Silty-loamy–loamy (about 12.5%) soils are the dominant soil textures. The main land uses in the study area comprise accordingly rangelands (66.5%), farmlands (33.16%), and bare lands (0.26%). The prevailed land covers in the study area include *Artemisia* + *Poa* species (34.86%), croplands (33.16%), *Poa* + *Medicago* species (25.69%), *Paliurus* + *Artemisia* species (6.01%), and bare lands (0.26%). Geologically, the study area covered by Marl and Shaleston (245 ha), Loos (2230 ha), and quaternary alluvial fans (120 ha).The variation of annual precipitation in the study area is about 75 mm with an average of 491 mm (Mohammad-Ebrahimi et al., 2015). The average annual temperature of the study area stands at 28 °C.

2.2. Methods

The methodological process of the current study is presented in Fig. 2. As shown, the flowchart comprises three main steps including: 1) data preparation; 2) modeling process (objective 1); 3) performance analysis consists of initial performance assessment (objective 2) and advanced performance assessment (objective 3 and 4).

2.2.1. Inventory map of gullies

The gully erosion inventory map was prepared using field surveys with a DGPS (Differential Global Positioning System) device. Series of linear and digitated gullies with U-shaped and V-shaped cross-sections with tens of meters in width and depth are evident in the study area, mostly located nearby roads and foot of the hills (Figs. 1 and 3). In total, 25 gullies are scattered in the study area with an area of about 105.88 ha including six digitated (64.45 ha) and 19 linear gullies (41.43 ha), where the locations of all 25 gullies were recorded, mapped as polygons, and then all the cells intersected by gullies (2647 pixels with a 20 m resolution as positive samples) were used for modeling. 70% of gullies were randomly selected for training (18 gullies; equivalently 1985 pixels) and the 30% rest were set aside to validate the built models (7 gullies; equivalently 662 pixels) (Youssef et al., 2015; Hussin et al., 2016). The same configuration was applied for negative points (non-gully areas) where the same number and percentage of negatives was used in calibration and validation procedures (Lombardo et al., 2014; Cama et al., 2016; Kornejady et al., 2017). As proposed by Conoscenti et al. (2014), the positive and negative training/test sets were altered three times in order to assess the robustness of the models (Fig. 4). For better graphical check, only positive training and test sets are presented.

2.2.2. Preparation of the conditioning factors

The main geo-environmental factors affect gully erosion are rainfall features such as intensity, period, and spatial distribution (Kheir et al., 2007; Magliulo, 2012; Capra et al., 2012), topography derived factors such as contributing drainage area, distance from ridges, slope steepness, slope aspect, and slope curvatures (Montgomery and Dietrich, 1992; Samani et al., 2009; Capra et al., 2012; Conoscenti et al., 2013), lithology and soil related properties and features such as erosivity, soil water content, soil texture, and sub-surface flow (Parras-Alcántara et al., 2016; Marzolff et al., 2011; El Maaoui et al., 2012) and land use/land cover (LU/LC) (Poesen et al., 2003; Takken et al., 2008;

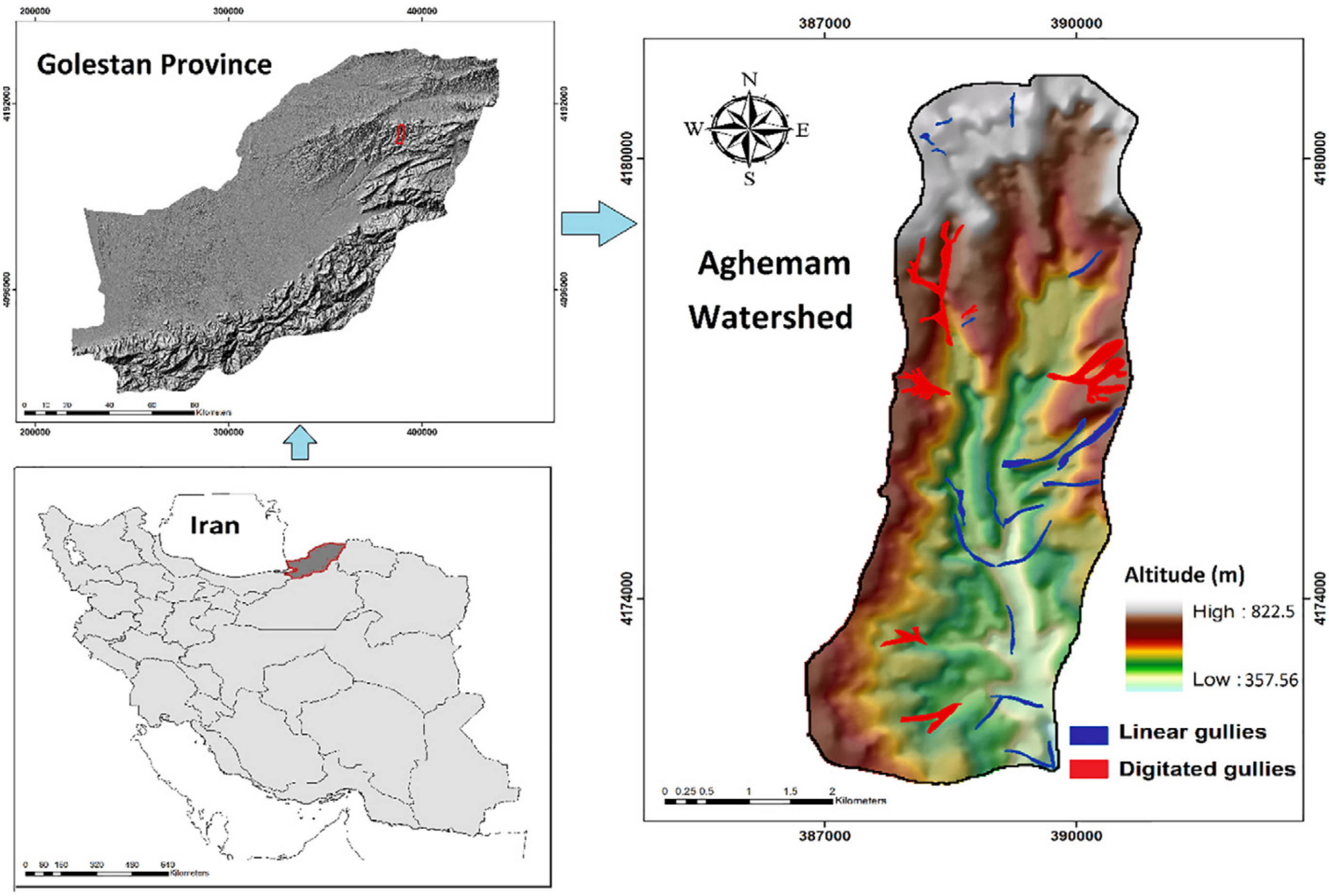

Fig. 1. The location of the study area in the Golestan Province and Iran.

Gómez-Gutiérrez et al., 2009a). In total, 16 gully conditioning factors were chosen including altitude (m), annual rainfall (mm), slope aspect, slope degree, slope-length (m), plan and profile curvatures (100/m), drainage density (km/km^2), topographic wetness index, distance from rivers (m), distance from roads (m), land cover (LC), land use (LU), lithological formations, soil texture, and hydrological units (Fig. S1) so that the selected agents covered the main well known and easily producible (in term of data availability) topo-hydrological and geo-environmental data. The preparation procedure of the factors is described as follow:

2.2.2.1. DEM derived factors. A DEM with a cell size of 20 × 20 m was created from 1:50,000-scale topographic contour map and obtained from Iranian National Cartographic Center (INCC). Roads and streams were extracted from this map. Correspondingly, slope aspect, slope degree, plan curvature, profile curvature, drainage density (using the actual drainage network of the study area), distance from streams, and distance from roads were mapped with the straight forward mathematical algorithms in the ArcGIS 10.2 environment. The slope-length map was produced following Eq. (1) (Moore and Burch, 1986):

$$LS = \left[FAG^{*}\frac{Cell-size}{22.13}\right]^{0.6} \times \left[\frac{Sin(slope-grid)^{*}0.01745}{0.0896}\right]^{1.3} \quad (1)$$

where, FAG is the flow accumulation grid and 0.01745 is a slope unit converter from radians to degree. The topographic wetness index (TWI) was mapped based on Eq. (2) (Beven and Kirkby, 1979):

$$TWI = \ln\frac{A_s}{tanb} \quad (2)$$

where, $A_s\alpha$ is the specific catchment area in m^2/m and b is the slope gradient (in degrees). The annual rainfall map (Fig. $S1_k$) of the study area was obtained from the Central Office of Natural Resources and Watershed Management of Golestan Province (CONRWMGP, 2007).

2.2.2.2. Categorical factors. The maps of the LU, LC, lithological formations, and soil texture (Fig. $S1_{i-o}$) of the study area were obtained from CONRWMGP (2007). The LC classes are described in Table 1. Accordingly, the hydrological unit map was prepared as the homogenous units consisted of LU map, related CN (Curve Number) values together with the soil texture and land cover information (Table 2). The map of lithological formations at the scale of 1:100,000 was acquired from Geological Survey Department of Iran (GSDI, 1997) consisted of three main units (Table 3). The soil textures of the study area comprise two main classes namely silty loamy and silty loamy-loamy soils (CONRWMGP, 2007).

At the end, it is important to check factors' multi-collinearity before gully susceptibility modeling to exclude highly correlated agents from modeling process and to avoid any resulted bias in models' results. Thus, variance inflation factor (VIF) was used in SPSS software to check this property. The VIF values > 5 connote that it is very likely to have a serious multi-collinearity between gully conditioning factors (O'brien, 2007). The inverse VIF is regarded as tolerance where the values < 0.1 indicate high multi-collinearity (Tien Bui et al., 2011).

2.3. Data mining models

2.3.1. Artificial neural network (ANN)

Artificial neural networks are machine learning models that imitate neural networks of the human body (Aleotti and Chowdhury, 1999;

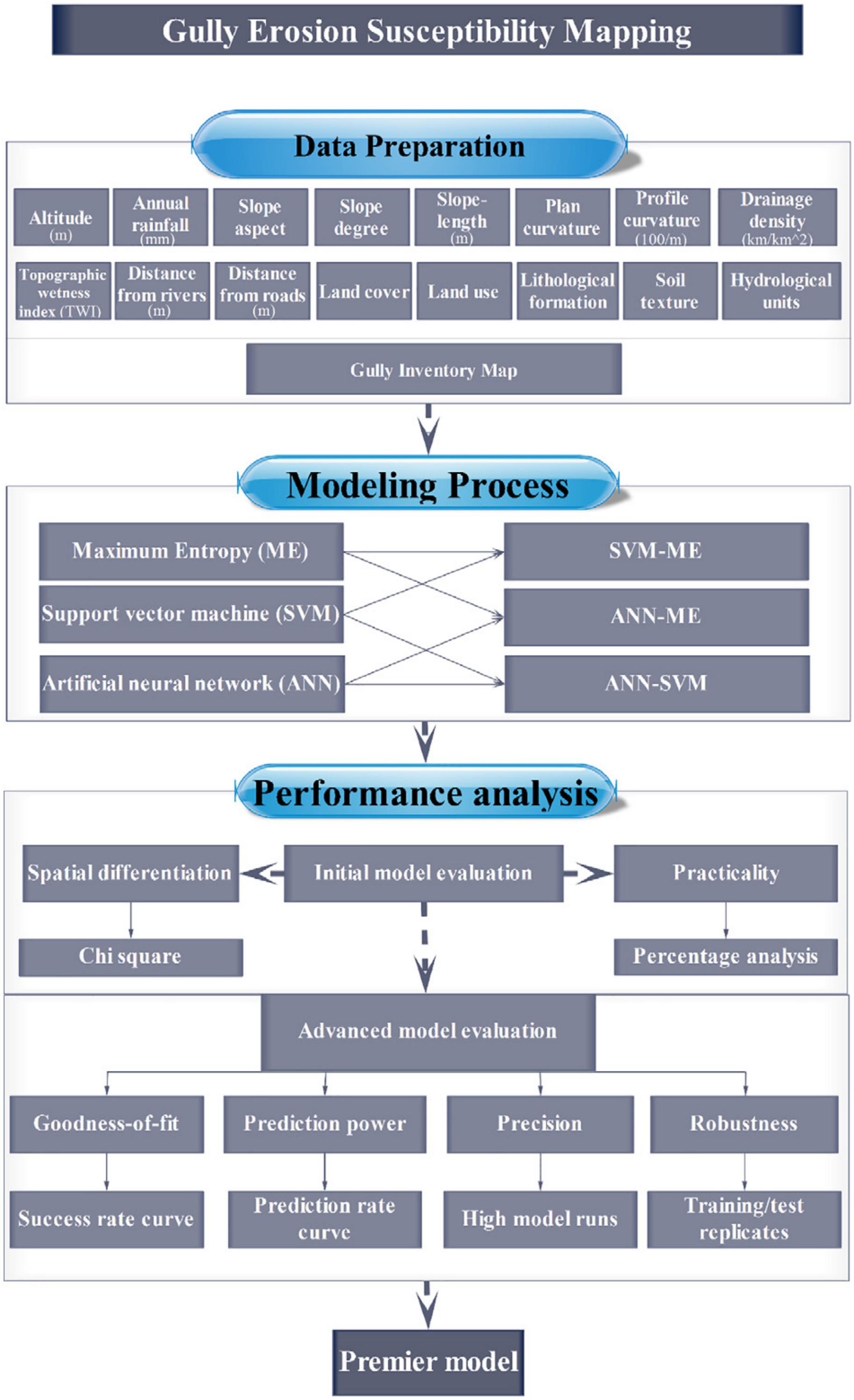

Fig. 2. Flowchart of the methodology used in the current study.

Tzeng and Ma, 2005; Cherkassky et al., 2006; Krasnopolsky, 2007). The ANNs include different algorithms capable of analyzing and predicting nonlinear property of a phenomenon (Peddle et al., 1994; Gong et al., 1996; Arora and Mathur, 2001; Saha et al., 2002). The multi-layer perceptron (MLP) is the most popular algorithm of the ANN (Kosko, 1992; Negnevitsky, 2002). Simply put, an MLP consists of nodes (neurons or processing elements) queued in three layers including the input layer, hidden layers, and the output layer. The nodes in hidden layer are responsible to analyze the complex information inside data while the input layer is passive and not sensitive enough to do so. In fact, the input layer comprises the conditioning factors and gully erosion training data and the output layer would be the gully erosion susceptibility map. So, the hidden and output layers actively work on generalization and prediction power of the model through taking the information (signals) from input nodes and processing the complex functions (Falaschi et al., 2009; Zare et al., 2013). The number of input and output nodes are fixed by a designed application in which the input nodes are equal to our gully conditioning factors and the output

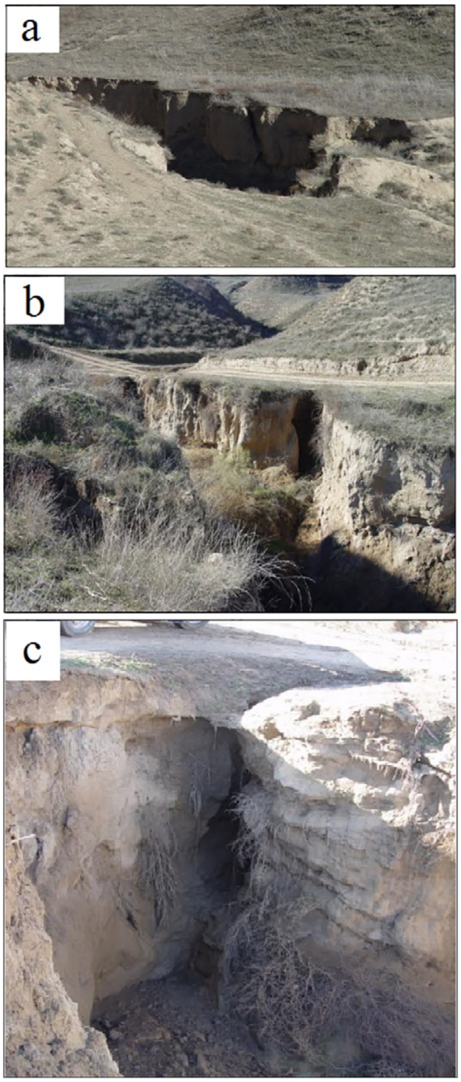

Fig. 3. Some photographs of the gullies scattered in the study area, a) a linear gully, b) a digitated gull erosion nearby the road, and c) a view of the gully headcut.

nodes are equal to a pair values (between 0 and 1) for each pixel: one for non-gully probability and the other for gully probability. The number of hidden layers and their nodes are determined by trial and error (Gong et al., 1996). Details can be found in different publications (Arora et al., 2004; Yesilnacar and Topal, 2005; Kanungo et al., 2006; Prasad et al., 2012; Dou et al., 2015).

2.3.2. Support vector machine (SVM)

Support vector machine is a discriminative supervised classifier which is based on statistical learning theory introduced by Vladimir and Vapnik (1995). SVM can be used for both classification and regression purposes (Cristianini and Shawe, 2000). It contains different types of classification functions capable of evaluating errors and generalizing information requiring minimum amount of model tuning (Joachims, 1998). These functions use the information stored inside factors in high iterations to capture the inherent complex behavior of a phenomenon (Burges, 1998). In general, the hyper-plane with the maximum margin would have the best classification performance (Kanevski et al., 2009). When facing real noisy objects, finding a sharp hyper-plane between objects is much harder than the theoretical view of the problem. So, a soft hyper-plane is set letting some training data cross over the margin with an acceptable empirical error (total distance of the training points from the margin) (Marjanović et al., 2011). The increase in model error will subsequently lead to increase in the model complexity (less fitted model) and decrease in generalization and vice versa. So, a unique n-dimensional hyper-plane solution with a maximum gap should be found that is complex enough and also has small training errors (Hastie et al., 2001). This solution depends only on a subset of training points as support vectors that contain sufficient information about classes (Tax and Duin, 1999).

In the current study, to cope with the non-linearity of the classification, we applied one of the most popular kernel functions called Radial Basic Function (RBF), more specifically Gaussian kernel (Cristianini and Shawe, 2000; Pourghasemi et al., 2013). The RBF can transform the non-linear classes into a linear one in high dimensional space (Poeppl et al., 2017; Marjanović et al., 2011) following the Eq. (3):

$$K(\mathrm{x},\mathrm{y}) = \exp\left(-\gamma\|X_i - X_j\|^2\right) \tag{3}$$

where, γ is the gamma parameter. Better estimation of the gamma parameter will make better results. We operate the SVM-RBF function using ksvm package in the R software to map gully erosion susceptibility in the study area.

2.3.3. Maximum entropy (MaxEnt)

MaxEnt is a presence-only general purpose machine learning model (Phillips et al., 2009; Quinn et al., 2013). The presence-only feature of the model is particularly important where facing impassable or remote areas (Keesstra et al., 2016), in which recording the phenomenon under study is impossible or costly. On the other hand, the model is exposed to biased data nearby accessible areas (Reddy and Dávalos, 2003; Austin, 2007; Raes and ter Steege, 2007; Veloz, 2009; Cao et al., 2016). Semantically, entropy is the expected value (average) of the information contained in our data (Shannon, 1948). MaxEnt lies in information theory and statistics in which it uses the presence localities of a phenomenon and a set of geo-environmental conditioning factors to estimate an unknown probability distribution. First, MaxEnt simply guesses that spatial probability of occurrence for the phenomenon (here gully erosion) is equal at the all pixels so that it chooses the uniform probability distribution function (pdf) as the target distribution. Then, some constraints force this pdf to the true target distribution. These constraints are extracted from those geo-environmental factors used in gully erosion susceptibility mapping. In fact, MaxEnt uses the interchangeable equation of those factors, so-called features, not the factors themselves (Elith et al., 2011). Different factors, form different features that impose specific constraints on the first guess of the MaxEnt. For instance, a continuous layer such as distance from streams forms a linear feature imposing a constraint on the empirical average of the factor values at the presence localities. If the mean value of the factor at the presence points is, for instance, equal to 102 m, MaxEnt will consider the locations close to this number as highly susceptible areas. There are other three features for continuous factors namely quadratic, product, and threshold and one for categorical factors viz *k* binary feature (Phillips et al., 2004). The maximum entropy would be the final best estimation which satisfies all the constraints (Jaynes, 1957a, b). More details on mathematical process are given in Phillips et al. (2004, 2009), and Elith et al. (2011).

2.4. Performance metrics

Performance of the models was assessed based on three levels: 1) initial statistics, 2) calibration, and 3) validation. As regards the initial statistics, the chi-square test between the susceptibility classes' percentages and the practicality of the models—as a measure of producing highly focused susceptibility maps in highly susceptible classes— were examined. The calibration was assessed using the AUSRC index (area under the success rate curve), by examining the goodness-of-fit of the models. SRCs (success rate curves) were made by plotting the

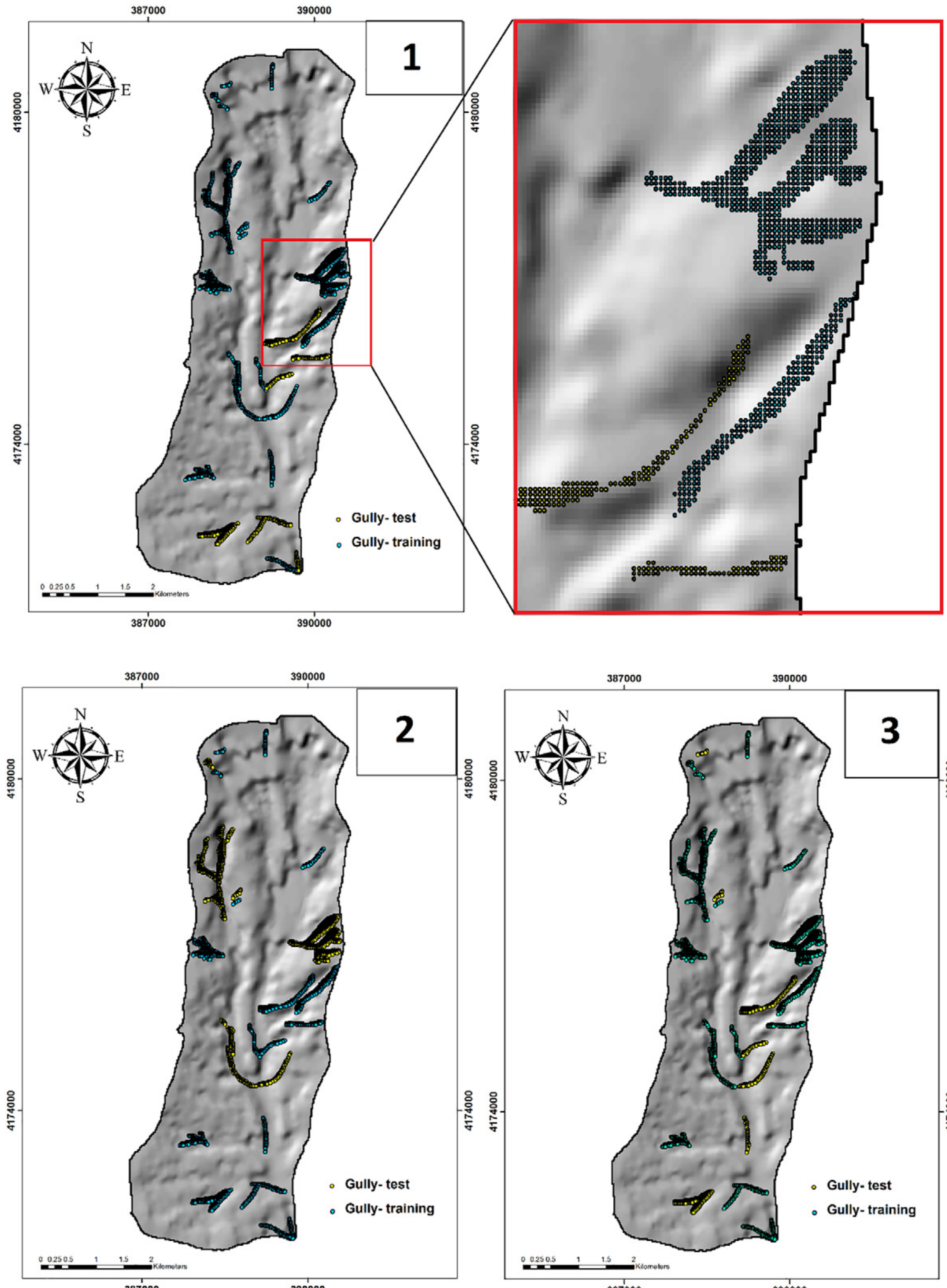

Fig. 4. Three 70:30 randomly split training and test replicates used for assessing the models' robustness.

cumulative percentage of susceptible areas (from the highest values to the lowest) on the X axis and the cumulative percentage of corresponding gully training set on the Y axis (Blahut et al., 2010). The validation task was carried out by assessing the prediction power, precision, and stability (robustness) of the models. The prediction power was assessed using the AUPRC index, as an indicator for generalization capacity. The PRCs (prediction rate curves) were calculated by plotting the cumulative percentage of susceptible areas against the cumulative percentage of the test set. The precision was evaluated by high model runs on calibration (training) set to reach precise results. This was set based on the predefined amount of runs correspond to each model and the visual check of the resulted AUSRCs. As mentioned earlier, the robustness of the models was tested by randomly altering the training-test sets three times and assessing the AUSRCs and AUPRCs for each model. We

Table 1
Description of land cover classes.

Land cover class	Description
Pa + Ar	Paliurus + Artemisia
Ar + Po	Artemisia + Poa
CL	Crop lands
Po + Me	Poa + Medicago
Ma	Bare lands

proposed a mathematical representation of the robustness following the expressions:

$$CI = |R_2 - R_1| + |R_3 - R_1| \tag{5}$$

$$SI = \frac{|CI_i - CI_{\max}|}{CI_{\max} - CI_{\min}} \tag{6}$$

where, CI is the change index, R_1, R_2, and R_3 are respectively the AUSRC or AUPRC values in first, second, and third replicates, $SI$is the stability index which follows a unity-based normalization method, and finally CI_i, $CI_{\min}$, and $CI_{\max}$ are respectively the ith, minimum, and maximum change index.

2.5. Ensemble modeling

Ensemble modeling, as a process of synthesizing the results of single models into a single incorporated model in order to boost the accuracy of predictive power (Rokach, 2010; Lee et al., 2012), has gained many interests among modelers especially those dealing with data mining models (Tien Bui et al., 2014; Jebur et al., 2014). Almost all the ensemble techniques (e.g. bagging and boosting) use the weighted integration of individual models to come up with the outcome. Though, the way of computing these weights are different. The current study handles an integration method known as heterogeneous category which uses the simple mathematics (multiplication, division, addition, and subtraction) where we proposed an improved equation which steps further. After running all three model, the following weighted mean expression was used to create ensemble models:

$$EM = \frac{\sum_{i=1}^{n} (AUSRC_i{}^{*} M_i)}{\sum_{i=1}^{n} AUSRC} \tag{4}$$

where, EM is the resulted ensemble model, $AUSRC_i$ is the $AUSRC$ value of the ith single model (M_i). By using such equation, the drawbacks of simple assumptions of abovementioned operators (e.g. simple averaging) are left behind since the resulted outcome of all models is not just a simple integration of the models, but resulted from assigning models' performance, more specifically their learning and fitting skill, as their weight and then synthesizing them via weighted averaging.

Table 2
Description of land use classes and the corresponding Curve Number (CN) values and hydrological units (Cronshey, 1986).

Land use class	CN value	Hydrological unit	Runoff generation potential
Agriculture	81	B	Medium
Agriculture	88	C	Relatively high
Agriculture	91	D	Very high
Bare land	86	B	Medium
Bare land	91	C	Relatively high
Range land	76	B	Medium
Range land	82	C	Relatively high
Range land	86	D	Very high

Table 3
Description of lithological formations in the study area.

Abbreviation	Geological system (Period)	Material description
KS	Cretaceous	Limestone, marl, and shale
OL	Quaternary	Loess
Qal	Quaternary	Alluvium

3. Results and discussion

3.1. Multicollinearity analysis, parameter assignment and running models

As regards the multi-collinearity values in Table 4, the highest VIF and the lowest tolerance values are about 3.98 and 0.251, respectively. The highest and the lowest VIF values are respectively related to slope degree (3.98) and slope aspect (1.128). Generally, the more independent factors we have in the model, the more likely we experience multi-collinearity issues. Nonetheless, the resulted VIF values indicate no multi-collinearity among the sixteen gully conditioning factors which permit us to include all the factors in the modeling process.

After preparing conditioning factors' maps (Fig. S1), we went through parameter assignment for the three main models ME, SVM, and ANN. To this aim, we used the user-specified parameters for ME model: 10,000 background points, 0.00001 as convergence threshold, 1000 times iteration and choosing "auto feature" to adjust the value of regularization parameter correspond to continuous and categorical layers. Further, we used SVM with a RBF algorithm tuning 1000 trees—to assure the adequacy issue— and three predictor variables as split points in each node. A multilayer perceptron (MLP) ANN with a feed forward back propagation algorithm was used consisting of 16 neurons in input layer (including gully conditioning factors), one hidden layer and one neuron in output layer. To find out the final number of neurons in the hidden layer we set 10 times model run through back propagation algorithm as to achieve the best fit on training data and highest model generalization (test set) which resulted in 10 neurons. Therefore, the final figuration of the network was set on 16 × 10 × 1. After assigning parameters for each model, the three separate models (ANN, SVM, and ME) (Fig. 5_{a-c}) and three ensemble models (ANN-SVM, ANN-ME, and SVM-ME) (Fig. 5_{d-f}) were produced and classified into four susceptibility classes namely low, moderate, high, and very high based on the natural break scheme (Hong et al., 2016;

Table 4
Multi-collinearity analysis for the gully conditioning factors using variance inflation factor (VIF).

Model	Collinearity statistics	
	Tolerance	VIF
SA	0.887	1.128
HU	0.255	3.908
DEM	0.276	3.613
LC	0.656	1.523
LF	0.737	1.357
SL	0.292	3.424
LU	0.673	1.486
Pl.C	0.473	2.115
Pr.C	0.802	1.246
AR	0.482	2.077
D.D	0.555	1.802
D.f.Ri	0.547	1.827
D.f.Ro	0.426	2.346
SD	0.251	3.983
ST	0.265	3.761
TWI	0.454	2.202

Description: (HU: hydrological units, ST: soil texture, D.f.Ro: distance from roads, SA: slope aspect, DEM: digital elevation model, D.f.Ri: distance from rivers, DD: drainage density, AR: annual rainfall, Pr.C: profile curvature, Pl.C: plan curvature, LU: land use, SL: slope length, LF: lithological formations, LC: land cover, TWI: topographic wetness index, and SD: slope degree).

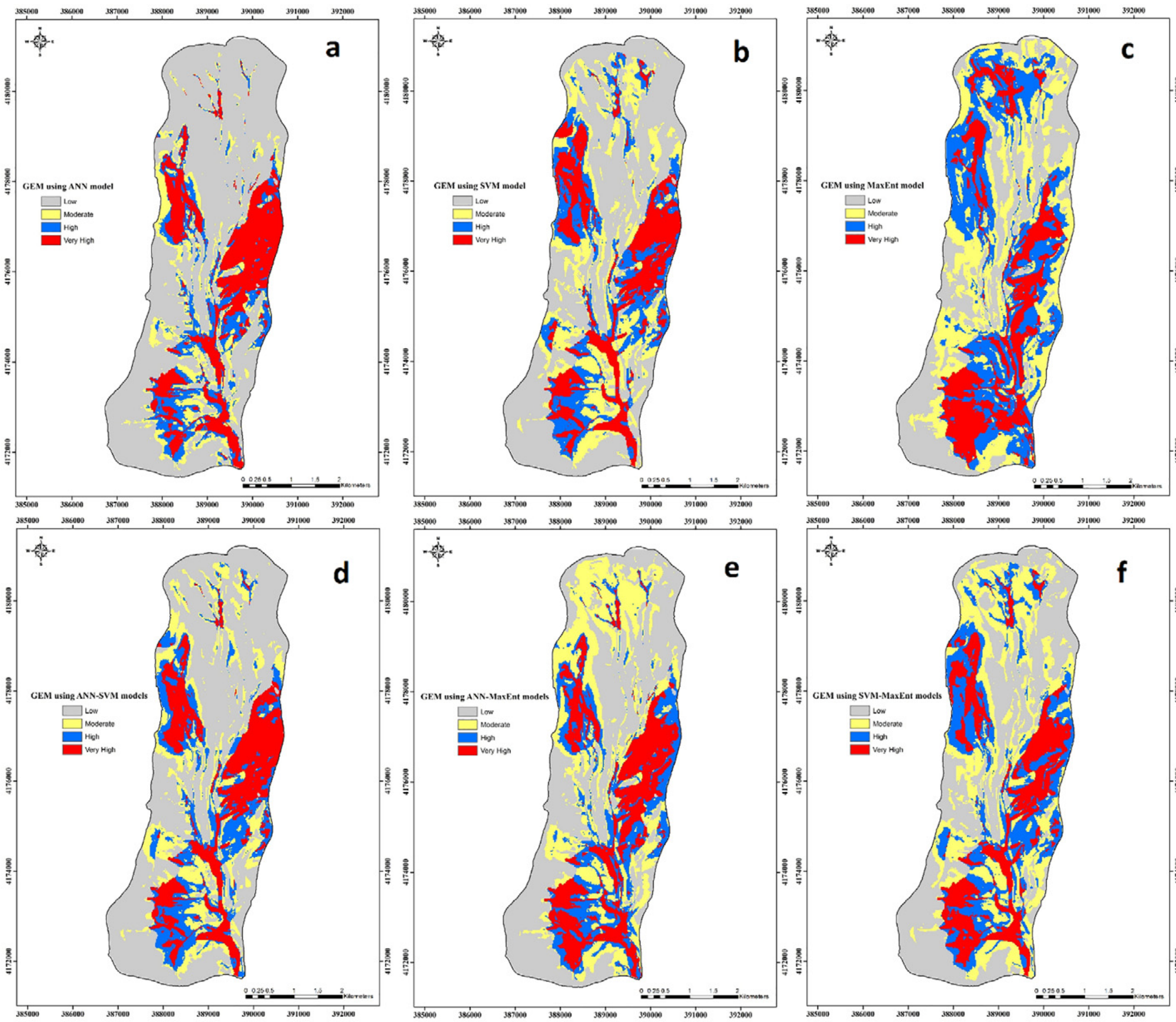

Fig. 5. Gully erosion susceptibility modelling using: a) ANN; b) SVM; c) MaxEnt; d) ANN-SVM; e) ANN-MaxEnt; and f) SVM-MaxEnt algorithms in the study area.

Pourghasemi and Rossi, 2016; Pourghasemi and Kerle, 2016; Rahmati et al., 2016b).

3.2. Initial inferences: concordance and practicality

Percentage of gully erosion susceptibility classes resulted from six models are summarized in Table 5. We ran the chi square test for models' classes in order to assess the concordance and see which model is reflecting the spatial differentiation of the gully erosion pattern better (Table 6). We used upward and downward arrows to show the reducer and increaser model when assembling them in order to depict clearer result. According to Table 6, all the models have acceptable values and successfully mirrored the differentiation in which chi square values are significant in 95% confidence level (P-value < 0.5). But in detail, ANN model has the highest chi square (36,656), while ME model has the lowest value (1772), and SVM is placed somewhere in middle (13,275). Hence, whenever models are combined with ANN as an ensemble model, their differentiation index is increasing which indicates the ANN model as an increaser. On the contrary, the ME is acting the opposite as a reducer model, increasing other models' performance in this regard. A Review on ensemble modeling in different literature (Chen et al., 2017), showed that this particular result happens when a model with higher performance is combined with an underperformed model. In other words, an outperformed and superior model can add positive properties to other subordinate models which appears as an

Table 5
Percentage of gully erosion susceptibility classes obtained from six separate and ensemble models (L: low; M: moderate; H: high; VH: very high).

Separate models	Susceptibility class	Percentage	Ensemble models	Susceptibility class	Percentage
ANN	L	57.37	ANN-SVM	L	48.57
	M	12.69		M	17.98
	H	11.63		H	15.44
	VH	18.31		VH	18.01
SVM	L	44.42	ANN-ME	L	39.02
	M	21.35		M	26.58
	H	16.57		H	16.36
	VH	17.66		VH	18.04
ME	L	25.98	SVM-ME	L	34.92
	M	29.17		M	27.04
	H	26.74		H	20.44
	VH	18.11		VH	17.60

Table 6
Concordance and behavior (practicality) indices for gully erosion susceptibility models.

Separate model	Concordance			Separate model	Behavior		
	Chi square	Ensemble model	Chi square		H + VH (%)	Ensemble model	H + VH (%)
ANN	**36,656**	ANN-SVM	19,194↓	ANN	29.94	ANN-SVM	33.45↓
		ANN-ME	8296↓			ANN-ME	34.40↑
SVM	13,275	ANN-SVM	19,194↑	SVM	*17.66 C*	ANN-SVM	33.45↑
		SVM-ME	4590↓			SVM-ME	38.04↑
ME	*1772*	ANN-ME	8296↑	ME	**44.86 A**	ANN-ME	34.40↓
		SVM-ME	4590↑			SVM-ME	38.04↓

Description: An upward arrow means that the chi square value of a model is increased after combining with another model and vice versa for a downward arrow. The bold and italic numbers indicate the respective highest and lowest values. The letters **A** and *C* stand for **Aggressive** and *Conservative* models. The significance of the chi square values within all models' classes is acceptable at 95% confidence level (P-value < 0.5).

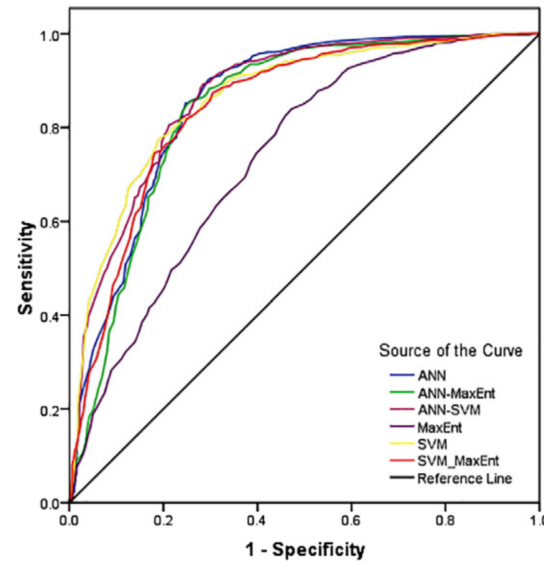

Fig. 6. Area under the success rate curve (AUSRC) correspond to ME, ANN, SVM, ANN-ME, SVM-ME, and ANN-SVM models in the study area.

improvement in results, when ensemble modeling is the case. This is also evident in advanced results on AUSRC and AUPRC (see Section 3.3). The ANN-SVM model achieved the second rank with a slight difference. The reducer role of ME in model ensemble results from some drawback of choosing background and presence localities where they can be polluted to biased data. The same exact result was reported by Chen et al. (2017) in which the abovementioned drawback has been deductively reasoned. Besides, the tradeoff between fitting and over-fitting (being highly focused, localized, and complicated with less generalization capacity at the same time), strongly depends on normalization parameter and convergence threshold so that they can also affect model generalization capacity and prediction power. However, ANN and SVM are not flawless either. For instance, ANN is known to act as a memorizing machine and holding on to local minima but here it could manage to be the superior single model among others which can be the results of selecting the MLP algorithm with proper backpropagation-forward learning. SVM as the best pattern recognition algorithm can occasionally encounter problems with solving high-dimensional and non-separable cases, but with RBF kernel function and enough model runs and parameter tuning it has apparently crossed this obstacle (Svoray et al., 2012).

Also, as summarized in Table 5, ME model is behaving aggressive in modeling the susceptibility pattern over the study area in which it minimizes the area of low and moderate classes and adds it to upper classes, recognizing about 45% of the study area as highly susceptible to gullying. This threatens the practicality of the model so that allocating pragmatic actions seems to be much harder and even impractical to this large area. In contrast, ANN-SVM ensemble model is showing conservative results considering about 34% of the watershed as highly susceptible areas. Regarding this criteria, the ME is an increaser model forcing other models to act aggressive and impractical when used within ensemble models and SVM as a reducer model inducing conservative properties to other models. In general, all models, be it separate or ensemble, unanimously agreed upon that 34% to 45% of the watershed is highly prone to gully erosion which is a sizeable number.

3.3. Advanced inferences: goodness-of-fit, predictive power, precision, and robustness

Comparing the AUSRC values of the single and ensemble models in Fig. 6 and Table 7 indicates the ensemble of ANN-SVM as the premier model with the highest fitting skill with a value of 0.889. In this regard, ME had the lowest fitting with a value of 0.735. Although the ensemble algorithm proposed for model integration could be the first guess for this result, this should be approved through all validation procedures since the ensemble might act differently or unstable compared to other ensembles or its single counterparts. Having a look at AUPRC values in Fig. 7 and Table 7 attests this result once again where the ensembles outperformed single models regarding prediction skill. The ANN-SVM ensemble had even higher prediction skill than that of other ensembles.

Regarding precision, all the single models had the suitable precision because their results are the product of high model runs. That is, the number of runs was tuned even much higher than what was designed as models' default configuration in such way that ensured the plateau effect (no changes in result anymore). This was set to 1000, 1000, and 100 runs respectively for ME, ANN, and SVM models. High runs were also applied to different replicates.

As presented in Table 7, ANN-SVM ensemble with the highest SI value—closer AUSRCs and AUPRCs in different replicates compared to other models— indicated a high agreement and robustness in its results, while other models showed asymmetries in their results. Especially, the ME model had the lowest stability in both AUSRC and AUPRC stability case. This connotes ME as a model with an unreliable results and a high sensitivity to different training/test replicates in the current study area. If models' performance are to be assessed based on their average AUSRC and AUPRC values through three replicates, the ANN-SVM would be the premier model all the way with the highest goodness-of-fit, prediction power, CI, and SI values.

3.4. Comparison of results

Since the model comparison and performance assessment of data mining models are the main objective o present study, a direct comparison of our results with findings of other studies is difficult due to different sampling strategies for training/test data partitioning, different spatial scales, different sets of predictors, and different model evaluation techniques. Despite the fact that data mining techniques have brought us valuable information on different scientific fields in an efficient amount of time rather than traditional methods, we still experience a sensible gap in the use of these methods especially in gully erosion susceptibility mapping, let alone ensemble modeling. Although there are some rare pieces of literature that have specifically dealt with model comparison and performance assessment.

Svoray et al. (2012) in a study on gully erosion at a catchment scale, compared data mining techniques with analytical hierarchy process (AHP) and traditional expert-based systems. As a result, the MLP-ANN and SVM-RBF techniques outperformed other models with higher AUC values and were selected as premier models for further studies on predicting gully initiation process. As an interdisciplinary survey, Phillips et al. (2004, 2009), and Phillips and Dudík (2008) worked

Table 7
Validation of models through three training/test replicates.

Models	AUSRC						AUPRC					
	Replicate 1	Replicate 2	Replicate 3	Avg.	CI	SI	Replicate 1	Replicate 2	Replicate 3	Avg.	CI	SI
ANN	0.856	0.832	0.811	0.833	0.069	0.612	0.847	0.810	0.850	0.836	0.040	0.545
ANN-MaxEnt	0.841	0.820	0.801	0.821	0.061	0.681	0.790	0.800	0.822	0.804	0.042	0.485
ANN-SVM	**0.889**	**0.910**	**0.892**	**0.897**	0.024	**1**	**0.871**	**0.879**	**0.888**	**0.879**	0.025	**1**
MaxEnt	0.735	0.640	0.780	0.718	0.140	0	0.690	0.640	0.703	0.681	0.053	0
SVM	0.862	0.880	0.820	0.854	0.060	0.690	0.845	0.811	0.821	0.826	0.058	0.132
SVM_MaxEnt	0.845	0.880	0.818	0.848	0.062	0.672	0.831	0.802	0.814	0.816	0.046	0.364

Descriptions: "Avg.", "CI" and "SI stand for respectively: "average", "change index", and "stability index". The bold values represent the highest ones among their counterparts.

immensely on the application of maximum entropy on species distribution assessment along with other scholar in landslide science (Kornejady et al., 2017) and ground water potential mapping (Rahmati et al., 2016b), where besides the favorable attributes of the model such as user-friendly, high run modeling capability, and acceptable accuracy, some serious drawbacks have been issued. Most importantly, the presence-only feature forces the model to choose some random background data in order to pave the fitting task and recognizing the phenomenon pattern in a specific area. Although feasible and practical, still problematic, because the model has to treat those backgrounds as pseudo-absences (no-occurrence) when plotting ROC curve (Kornejady et al., 2017) which is clearly in conflict with the main objective of the model, this being presence-only evaluation (Guillera-Arroita et al., 2014). So that, the scholars themselves admitted to this flaw and have not given a straight forward and an easy solution to cope with it, except for choosing background data more wisely through immense field surveys (Phillips and Dudík, 2008).

Kornejady et al. (2017) tested Mahalanobis distance method to specifically deal with boosting ME results by wisely partitioning training/test data sets. Nonetheless, also add anti-data bias works and dealing with parameters amalgamation to problems above. Zakerinejad and Märker (2014) reported a very well performance of ME on gully susceptibility mapping in southwest Iran; however, no model comparison was conducted to genuinely test the ME applicability and accuracy. Although the issues above may be overwhelmed by both ANN and SVM too, powerful supplemental techniques of MLP for ANN (high runs of back and forth learning and great memorizing ability) and RBF for SVM (powerful pattern recognition especially in high-dimensional problems) have excelled ME in learning and generalization missions. These properties have also been reported by Pourghasemi et al. (2013), Tsangaratos and Benardos (2014), and Chen et al. (2017).

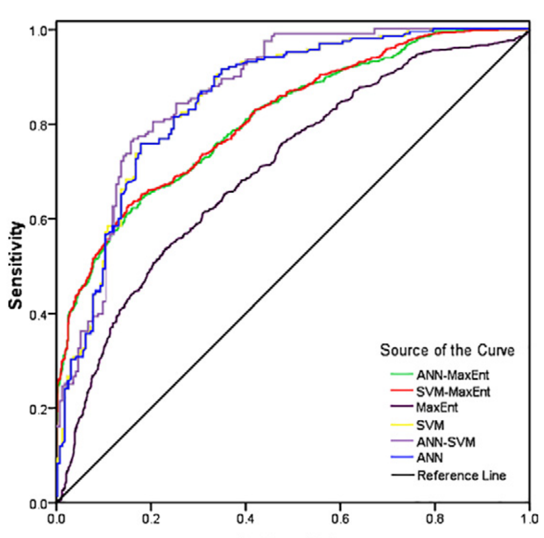

Fig. 7. Area under the prediction rate curve (AUPRC) correspond to ME, ANN, SVM, ANN-ME, SVM-ME, and ANN-SVM models in the study area.

Conoscenti et al. (2014) was the pioneer as for robustness and precision assessments on gully susceptibility modeling, where the logistic regression analyses were conducted through different data replications. Although the differences in our models make comparison impossible, the proposed stability indices can be compared in future works.

4. Conclusion

The context of gully erosion susceptibility mapping is a crucial area of interest in the watersheds prone to this destructive phenomenon. The Aaghemam Watershed is one of the most susceptible areas to gullying in the Golestan Province due to owning collection of gully conditioning factors with a footprint of man-made interruptions. Indeed, it is a mission to provide a more understandable platform to inform decision makers about the current situation of this study area as much as conceivable. So, what follows is the conclusion of the present study:

I. As regards the model results, ANN and SVM play an improver role when combines with other models as an ensemble model since they has improved the AUSRC and AUPRC values, while ME appeared to be a depriver. This might be caused by the algorithm used by the models whereas ANNs are benefited by back and forth propagation learning algorithms which help the model learn and progress. Similarly, SVM with a radial basis function helped the models recognize the gullying pattern. The background pseudo-absence sampling and the probable biased process resulted from ME mechanism might be one of the main reason for the ME underperformance. Also, ME found to be hard to configure the parameter settings which makes it more black-box compared to ANN and SVM.
II. Ensemble modeling proved to be a suitable technique to outperform the single models whereas ANN and SVM congruently helped each other improve. This might be resulted from their highly AUSRC and AUPRC values. So, the combination of SVM and ANNs algorithms in the form of a new data mining model could be promising in future studies.
III. Regarding the robustness results, the ANN-SVM ensemble had the highest stability in its results where the highest agreement between AUSRC and AUPRC values was founded in different training/test replicates. Contrarily, other models especially single ones had asymmetries in their results which is a sign of instability and unreliability.

Supplementary data to this article can be found online at http://dx.doi.org/10.1016/j.scitotenv.2017.07.198.

References

Akgün, A., Türk, N., 2011. Mapping erosion susceptibility by a multivariate statistical method: a case study from the Ayvalık region, NW Turkey. Comput. Geosci. 37 (9), 1515–1524.

Aleotti, P., Chowdhury, R., 1999. Landslide hazard assessment: summary review and new perspectives. Bull. Eng. Geol. Environ. 58 (1), 21–44.

Ariyanto, A.C., 2015. Mapping of Possible Corridors for Javan Leopard (*Panthera pardus* ssp. melas) Between Gunung Merapi and Gunung Merbabu National Parks, Indonesia. Doctoral dissertation. University of Twente.
Arora, M.K., Das Gupta, A.S., Gupta, R.P., 2004. An artificial neural network approach for landslide hazard zonation in the Bhagirathi (Ganga) Valley, Himalayas. Int. J. Remote Sens. 25 (3), 559–572.
Arora, M.K., Mathur, S., 2001. Multi-source classification using artificial neural network in a rugged terrain. Geocarto Int. 16 (3), 37–44.
Austin, M., 2007. Species distribution models and ecological theory: a critical assessment and some possible new approaches. Ecol. Model. 200 (1), 1–19.
Beven, K.J., Kirkby, M.J., 1979. A physically based, variable contributing area model of basin hydrology/Un modèle à base physique de zone d'appel variable de l'hydrologie du bassin versant. Hydrol. Sci. J. 24 (1), 43–69.
Billi, P., Dramis, F., 2003. Geomorphological investigation on gully erosion in the Rift Valley and the northern highlands of Ethiopia. Catena 50 (2), 353–368.
Blahut, J., van Westen, C.J., Sterlacchini, S., 2010. Analysis of landslide inventories for accurate prediction of debris-flow source areas. Geomorphology 119 (1), 36–51.
Burges, C.J., 1998. A tutorial on support vector machines for pattern recognition. Data Min. Knowl. Disc. 2 (2), 121–167.
Buttafuoco, G., Conforti, M., Aucelli, P.P.C., Robustelli, G., Scarciglia, F., 2012. Assessing spatial uncertainty in mapping soil erodibility factor using geostatistical stochastic simulation. Environ. Earth Sci. 66 (4), 1111–1125.
Cama, M., Conoscenti, C., Lombardo, L., Rotigliano, E., 2016. Exploring relationships between grid cell size and accuracy for debris-flow susceptibility models: a test in the Giampilieri catchment (Sicily, Italy). Environ. Earth Sci. 75 (3), 1–21.
Cao, B., Bai, C., Zhang, L., Li, G., Mao, M., 2016. Modeling habitat distribution of Cornus officinalis with Maxent modeling and fuzzy logics in China. J. Plant Ecol. rtw009.
Capra, A., Ferro, V., Porto, P., Scicolone, B., 2012. Quantifying interrill and ephemeral gully erosion in a small Sicilian basin interrill and ephemeral gully erosion in a small Sicilian basin. Z. Geomorphol. 56 (1), 9–25 Supplementary Issues.
Central Office of Natural Resources and Watershed Management in Golestan Province (CONRWMGP), 2007. Detailed Action Plan of Ziarat Watershed. Pazhouhab Sharq Consulting Engineers Co, Iran.
Chaplot, V., Giboire, G., Marchand, P., Valentin, C., 2005a. Dynamic modelling for linear erosion initiation and development under climate and land-use changes in northern Laos. Catena 63 (2), 318–328.
Chaplot, V., Le Brozec, E.C., Silvera, N., Valentin, C., 2005b. Spatial and temporal assessment of linear erosion in catchments under sloping lands of northern Laos. Catena 63 (2), 167–184.
Chen, W., Pourghasemi, H.R., Kornejady, A., Zhang, N., 2017. Landslide spatial modeling: introducing new ensembles of ANN, MaxEnt, and SVM machine learning techniques. Geoderma 305, 314–327.
Cherkassky, V., Krasnopolsky, V., Solomatine, D.P., Valdes, J., 2006. Computational intelligence in earth sciences and environmental applications: issues and challenges. Neural Netw. 19 (2), 113–121.
Comino, J.R., Quiquerez, A., Follain, S., Raclot, D., Le Bissonnais, Y., Casalí, J., ... Pereira, P., 2016. Soil erosion in sloping vineyards assessed by using botanical indicators and sediment collectors in the Ruwer-Mosel valley. Agric. Ecosyst. Environ. 233, 158–170.
Conforti, M., Aucelli, P.P., Robustelli, G., Scarciglia, F., 2011. Geomorphology and GIS analysis for mapping gully erosion susceptibility in the Turbolo stream catchment (Northern Calabria, Italy). Nat. Hazards 56 (3), 881–898.
Conoscenti, C., Agnesi, V., Angileri, S., Cappadonia, C., Rotigliano, E., Märker, M., 2013. A GIS-based approach for gully erosion susceptibility modelling: a test in Sicily, Italy. Environ. Earth Sci. 70 (3), 1179–1195.
Conoscenti, C., Angileri, S., Cappadonia, C., Rotigliano, E., Agnesi, V., Märker, M., 2014. Gully erosion susceptibility assessment by means of GIS-based logistic regression: a case of Sicily (Italy). Geomorphology 204, 399–411.
Cristianini, N., Shawe, Taylor J., 2000. An Introduction to Support Vector Machines and Other Kernel-based Learning Methods. Cambridge University Press.
Cronshey, R., 1986. Urban Hydrology for Small Watersheds. US Dept. of Agriculture, Soil Conservation Service, Engineering Division.
Davis, J., Blesius, L., 2015. A hybrid physical and maximum-entropy landslide susceptibility model. Entropy 17 (6), 4271–4292.
Dickson, M.E., Perry, G.L., 2016. Identifying the controls on coastal cliff landslides using machine-learning approaches. Environ. Model. Softw. 76, 117–127.
Dou, J., Yamagishi, H., Pourghasemi, H.R., Yunus, A.P., Song, X., Xu, Y., Zhu, Z., 2015. An integrated artificial neural network model for the landslide susceptibility assessment of Osado Island, Japan. Nat. Hazards 78 (3), 1749–1776.
Dube, F., Nhapi, I., Murwira, A., Gumindoga, W., Goldin, J., Mashauri, D.A., 2014. Potential of weight of evidence modelling for gully erosion hazard assessment in Mbire District–Zimbabwe. Phys. Chem. Earth Parts A/B/C 67, 145–152.
El Maaoui, M.A., Felfoul, M.S., Boussema, M.R., Snane, M.H., 2012. Sediment yield from irregularly shaped gullies located on the Fortuna lithologic formation in semi-arid area of Tunisia. Catena 93, 97–104.
Elith, J., Phillips, S.J., Hastie, T., Dudík, M., Chee, Y.E., Yates, C.J., 2011. A statistical explanation of MaxEnt for ecologists. Divers. Distrib. 17 (1), 43–57.
Falaschi, F., Giacomelli, F., Federici, P.R., Puccinelli, A., Avanzi, G.A., Pochini, A., Ribolini, A., 2009. Logistic regression versus artificial neural networks: landslide susceptibility evaluation in a sample area of the Serchio River valley, Italy. Nat. Hazards 50 (3), 551–569.
Flanagan, D.C., Nearing, M.A., 1995. USDA-Water Erosion Prediction Project: Hillslope Profile and Watershed Model Documentation. Vol. 10 (NSERL report).
Fourcade, Y., Engler, J.O., Rödder, D., Secondi, J., 2014. Mapping species distributions with MAXENT using a geographically biased sample of presence data: a performance assessment of methods for correcting sampling bias. PLoS One 9 (5), e97122.
Geological Survey Department of Iran (GSDI), 1997. http://www.gsi.ir/Main/Lang_en/index.html.
Gómez-Gutiérrez, Á., Conoscenti, C., Angileri, S.E., Rotigliano, E., Schnabel, S., 2015. Using topographical attributes to evaluate gully erosion proneness (susceptibility) in two Mediterranean basins: advantages and limitations. Nat. Hazards 79 (1), 291–314.
Gómez-Gutiérrez, Á., Schnabel, S., Contador, F.L., 2009a. Gully erosion, land use and topographical thresholds during the last 60 years in a small rangeland catchment in SW Spain. Land Degrad. Dev. 20 (5), 535.
Gómez-Gutiérrez, Á., Schnabel, S., Contador, J.F.L., 2009b. Using and comparing two nonparametric methods (CART and MARS) to model the potential distribution of gullies. Ecol. Model. 220 (24), 3630–3637.
Gong, P., Pu, R., Chen, J., 1996. Elevation and forest-cover data using neural networks. Photogramm. Eng. Remote. Sens. 62 (11), 1249–1260.
Guillera-Arroita, G., Lahoz-Monfort, J.J., Elith, J., 2014. Maxent is not a presence–absence method, a comment on Thibaud et al. Methods Ecol. Evol. 5 (11), 1192–1197.
Hastie, T., Tibshirani, R., Friedman, J.H., 2001. The Elements of Statistical Learning: Data Mining, Inference, and Prediction. Springer Verlag, New York.
Hong, H., Naghibi, S.A., Pourghasemi, H.R., Pradhan, B., 2016. GIS-based landslide spatial modeling in Ganzhou City, China. Arab. J. Geosci. 9 (2), 1–26.
Hussin, H.Y., Zumpano, V., Reichenbach, P., Sterlacchini, S., Micu, M., van Westen, C., Bălteanu, D., 2016. Different landslide sampling strategies in a grid-based bi-variate statistical susceptibility model. Geomorphology 253, 508–523.
Jaynes, E.T., 1957a. Information theory and statistical mechanics. Phys. Rev. 106 (4), 620.
Jaynes, E.T., 1957b. Information theory and statistical mechanics. II. Phys. Rev. 108 (2), 171.
Jebur, M.N., Pradhan, B., Tehrany, M.S., 2014. Optimization of landslide conditioning factors using very high-resolution airborne laser scanning (LiDAR) data at catchment scale. Remote Sens. Environ. 152, 150–165.
Joachims, T., 1998. Text categorization with support vector machines: learning with many relevant features. European Conference on Machine Learning. Springer Berlin Heidelberg, pp. 137–142.
Kanevski, M., Pozdnoukhov, A., Timonin, V., 2009. Machine Learning for Spatial Environmental Data: Theory, Applications, and Software. EPFL Press, Lausanne (368 pp).
Kanungo, D.P., Arora, M.K., Sarkar, S., Gupta, R.P., 2006. A comparative study of conventional, ANN black box, fuzzy and combined neural and fuzzy weighting procedures for landslide susceptibility zonation in Darjeeling Himalayas. Eng. Geol. 85 (3), 347–366.
Keesstra, S., Pereira, P., Novara, A., Brevik, E.C., Azorin-Molina, C., Parras-Alcántara, L., ... Cerdà, A., 2016. Effects of soil management techniques on soil water erosion in apricot orchards. Sci. Total Environ. 551, 357–366.
Kheir, R.B., Wilson, J., Deng, Y., 2007. Use of terrain variables for mapping gully erosion susceptibility in Lebanon. Earth Surf. Process. Landf. 32 (12), 1770–1782.
Kim, H.G., Lee, D.K., Park, C., Kil, S., Son, Y., Park, J.H., 2015. Evaluating landslide hazards using RCP 4.5 and 8.5 scenarios. Environ. Earth Sci. 73 (3), 1385–1400.
Knisel, W.G., 1980. CREAMS: A Field Scale Model for Chemicals, Runoff, and Erosion From Agricultural Management Systems [USA]. Department of Agriculture. Conservation research report (USA), United States.
Kornejady, A., Heidari, K., Nakhavali, M., 2015. Assessment of landslide susceptibility, semi-quantitative risk and management in the Ilam dam basin, Ilam, Iran. Environ. Resour. Res. 3 (1), 85–109.
Kornejady, A., Ownegh, M., Bahremand, A., 2017. Landslide susceptibility assessment using maximum entropy model with two different data sampling methods. Catena 152, 144–162.
Kosko, B., 1992. Neural Networks and Fuzzy Systems: A Dynamical Systems Approach to Machine Intelligence/Book and Disk. Prentice Hall, Upper Saddle River.
Krasnopolsky, V.M., 2007. Neural network emulations for complex multidimensional geophysical mappings: applications of neural network techniques to atmospheric and oceanic satellite retrievals and numerical modeling. Rev. Geophys. 45 (3).
Kuhnert, P.M., Henderson, A.K., Bartley, R., Herr, A., 2010. Incorporating uncertainty in gully erosion calculations using the random forests modelling approach. Environmetrics 21 (5), 493–509.
Lee, M.J., Choi, J.W., Oh, H.J., Won, J.S., Park, I., Lee, S., 2012. Ensemble-based landslide susceptibility maps in Jinbu area, Korea. Environ. Earth Sci. 67, 23–37.
Lombardo, L., Cama, M., Maerker, M., Rotigliano, E., 2014. A test of transferability for landslides susceptibility models under extreme climatic events: application to the Messina 2009 disaster. Nat. Hazards 74 (3), 1951–1989.
Lucà, F., Conforti, M., Robustelli, G., 2011. Comparison of GIS-based gullying susceptibility mapping using bivariate and multivariate statistics: Northern Calabria, South Italy. Geomorphology 134 (3), 297–308.
Magliulo, P., 2012. Assessing the susceptibility to water-induced soil erosion using a geomorphological, bivariate statistics-based approach. Environ. Earth Sci. 67 (6), 1801–1820.
Marjanović, M., Kovačević, M., Bajat, B., Voženílek, V., 2011. Landslide susceptibility assessment using SVM machine learning algorithm. Eng. Geol. 123 (3), 225–234.
Märker, M., Pelacani, S., Schröder, B., 2011. A functional entity approach to predict soil erosion processes in a small Plio-Pleistocene Mediterranean catchment in Northern Chianti, Italy. Geomorphology 125 (4), 530–540.
Marzolff, I., Ries, J.B., Poesen, J., 2011. Short-term vs. medium-term monitoring for detecting gully-erosion variability in a Mediterranean environment: addressing the time-scale problem in gully dynamics. Geophysical Research Abstracts. Vol. 13, p. 11239.
Maslov, B.S., 2005. Agricultural Land Improvement: Amelioration and Reclamation. 1. Russian Academy of Agriculture Sciences, Russia, pp. 1–9.
Mekonnen, M., Keesstra, S.D., Baartman, J.E., Stroosnijder, L., Maroulis, J., 2017. Reducing Sediment Connectivity Through man-Made and Natural Sediment Sinks in the Minizr Catchment, Northwest Ethiopia. Land Degrad. Dev. 28 (2), 708–717.
Mohammad-Ebrahimi, M., Javadi, M.R., Vafakhah, M., 2015. Investigation of the role of soil and non-soil parameters in development of linear gully erosion in Aghemam watershed. Iran. J. Soil Sci. 29 (4), 487–498 (In Persian).
Montgomery, D.R., Dietrich, W.E., 1992. Channel initiation and the problem of landscape scale. Science 255 (5046), 826.
Moonjun, R., 2007. Application of Artificial Neural Network and Decision Tree in a GIS–based Predictive Soil Mapping for Landslide Vulnerability Study: A Case Study of Hoi Num Rin Sub–Watershed, Thailand. 104. ITC, Enschede.
Moore, I.D., Burch, G.J., 1986. Physical basis of the length-slope factor in the Universal Soil Loss Equation. Soil Sci. Soc. Am. J. 50 (5), 1294–1298.

Nefeslioglu, H.A., Sezer, E., Gokceoglu, C., Bozkir, A.S., Duman, T.Y., 2010. Assessment of landslide susceptibility by decision trees in the metropolitan area of Istanbul, Turkey. Math. Probl. Eng. 2010.

Negnevitsky, M., 2002. Artificial Intelligence—A Guide to Intelligent Systems. Addison-Wesley Co, Great Britain.

O'brien, R.M., 2007. A caution regarding rules of thumb for variance inflation factors. Qual. Quant. 41 (5), 673–690.

Pacheco, F.A.L., Varandas, S.G.P., Sanches Fernandes, L.F., Valle Junior, R.F., 2014. Soil losses in rural watersheds with environmental land use conflicts. Sci. Total Environ. 485-486C, 110–120.

Parras-Alcántara, L., Lozano-García, B., Keesstra, S., Cerdà, A., Brevik, E.C., 2016. Long-term effects of soil management on ecosystem services and soil loss estimation in olive grove top soils. Sci. Total Environ. 571, 498–506.

Peddle, D.R., Foody, G.M., Zhang, A., Franklin, S.E., LeDrew, E.F., 1994. Multi-source image classification II: an empirical comparison of evidential reasoning and neural network approaches. Can. J. Remote. Sens. 20 (4), 396–407.

Phillips, S.J., Dudík, M., Elith, J., Graham, C.H., Lehmann, A., Leathwick, J., Ferrier, S., 2009. Sample selection bias and presence-only distribution models: implications for background and pseudo-absence data. Ecol. Appl. 19 (1), 181–197.

Phillips, S.J., Dudík, M., Schapire, R.E., 2004. A maximum entropy approach to species distribution modeling. Proceedings of the Twenty-first International Conference on Machine Learning. ACM, p. 83.

Phillips, S.J., Dudík, M., 2008. Modeling of species distributions with Maxent: new extensions and a comprehensive evaluation. Ecography 31 (2), 161–175.

Poeppl, R.E., Keesstra, S.D., Maroulis, J., 2017. A conceptual connectivity framework for understanding geomorphic change in human-impacted fluvial systems. Geomorphology 277, 237–250.

Poesen, J., Nachtergaele, J., Verstraeten, G., Valentin, C., 2003. Gully erosion and environmental change: importance and research needs. Catena 50 (2), 91–133.

Pourghasemi, H.R., Jirandeh, A.G., Pradhan, B., Xu, C., Gokceoglu, C., 2013. Landslide susceptibility mapping using support vector machine and GIS at the Golestan Province, Iran. J. Earth Syst. Sci. 122 (2), 349–369.

Pourghasemi, H.R., Kerle, N., 2016. Random forests and evidential belief function-based landslide susceptibility assessment in Western Mazandaran Province, Iran. Environ. Earth Sci. 75 (3), 1–17.

Pourghasemi, H.R., Rossi, M., 2016. Landslide susceptibility modeling in a landslide prone area in Mazandarn Province, north of Iran: a comparison between GLM, GAM, MARS, and M-AHP methods. Theoretical and Applied Climatology, pp. 1–25.

Pradhan, B., 2013. A comparative study on the predictive ability of the decision tree, support vector machine and neuro-fuzzy models in landslide susceptibility mapping using GIS. Comput. Geosci. 51, 350–365.

Prasad, R., Pandey, A., Singh, K.P., Singh, V.P., Mishra, R.K., Singh, D., 2012. Retrieval of spinach crop parameters by microwave remote sensing with back propagation artificial neural networks: a comparison of different transfer functions. Adv. Space Res. 50 (3), 363–370.

Quinn, S.A., Gibbs, J.P., Hall, M.H., Petokas, P.J., 2013. Multiscale factors influencing distribution of the eastern hellbender salamander (Cryptobranchus alleganiensis alleganiensis) in the northern segment of its range. J. Herpetol. 47 (1), 78–84.

Raes, N., ter Steege, H., 2007. A null-model for significance testing of presence-only species distribution models. Ecography 30 (5), 727–736.

Rahmati, O., Haghizadeh, A., Pourghasemi, H.R., Noormohamadi, F., 2016a. Gully erosion susceptibility mapping: the role of GIS-based bivariate statistical models and their comparison. Nat. Hazards 82 (2), 1231–1258.

Rahmati, O., Pourghasemi, H.R., Melesse, A.M., 2016b. Application of GIS-based data driven random forest and maximum entropy models for groundwater potential mapping: a case study at Mehran Region, Iran. Catena 137, 360–372.

Reddy, S., Dávalos, L.M., 2003. Geographical sampling bias and its implications for conservation priorities in Africa. J. Biogeogr. 30 (11), 1719–1727.

Ren, F., Wu, X., Zhang, K., Niu, R., 2015. Application of wavelet analysis and a particle swarm-optimized support vector machine to predict the displacement of the Shuping landslide in the Three Gorges, China. Environ. Earth Sci. 73 (8), 4791–4804.

Rokach, L., 2010. Ensemble-based classifiers. Artif. Intell. Rev. 33, 1–39.

Saha, A.K., Gupta, R.P., Arora, M.K., 2002. GIS-based landslide hazard zonation in the Bhagirathi (Ganga) valley, Himalayas. Int. J. Remote Sens. 23 (2), 357–369.

Samani, A.N., Ahmadi, H., Jafari, M., Boggs, G., Ghoddousi, J., Malekian, A., 2009. Geomorphic threshold conditions for gully erosion in Southwestern Iran (Boushehr-Samal watershed). J. Asian Earth Sci. 35 (2), 180–189.

Shannon, C.E., 1948. A mathematical theory of communication, bell system technical journal 27: 379–423 and 623–656. Math. Rev. (MathSciNet: MR10, 133e).

Svoray, T., Michailov, E., Cohen, A., Rokah, L., Sturm, A., 2012. Predicting gully initiation: comparing data mining techniques, analytical hierarchy processes and the topographic threshold. Earth Surf. Process. Landf. 37 (6), 607–619.

Takken, I., Croke, J., Lane, P., 2008. Thresholds for channel initiation at road drain outlets. Catena 75 (3), 257–267.

Tax, D.M., Duin, R.P., 1999. Support vector domain description. Pattern Recogn. Lett. 20 (11), 1191–1199.

Tien Bui, D., Lofman, O., Revhaug, I., Dick, O., 2011. Landslide susceptibility analysis in the Hoa Binh province of Vietnam using statistical index and logistic regression. Nat. Hazards 59 (3), 1413–1444.

Tien Bui, D., Pradhan, B., Revhaug, I., Tran, C.T., 2014. A Comparative Assessment Between the Application of Fuzzy Unordered Rules Induction Algorithm and J48 Decision Tree Models in Spatial Prediction of Shallow Landslides at Lang Son City. Springer International Publishing, Vietnam.

Tien Bui, D., Tuan, T.A., Klempe, H., Pradhan, B., Revhaug, I., 2016. Spatial prediction models for shallow landslide hazards: a comparative assessment of the efficacy of support vector machines, artificial neural networks, kernel logistic regression, and logistic model tree. Landslides 13 (2), 361–378.

Tsangaratos, P., Benardos, A., 2014. Estimating landslide susceptibility through an artificial neural network classifier. Nat. Hazards 74 (3), 1489–1516.

Tzeng, F.Y., Ma, K.L., 2005. Opening the black box-data driven visualization of neural networks. VIS 05. IEEE Visualization. IEEE, pp. 383–390.

Umar, Z., Pradhan, B., Ahmad, A., Jebur, M.N., Tehrany, M.S., 2014. Earthquake induced landslide susceptibility mapping using an integrated ensemble frequency ratio and logistic regression models in West Sumatera Province, Indonesia. Catena 118, 124–135.

USDA-SCS, 1966. Procedure for Determining Rates of Land Damage, Land Depreciation, and Volume of Sediment Produced by Gully Erosion. Technical Release No. 32. US GPO 1990-261-419:20727/SCS. US Government Printing Office, Washington, DC.

Valera, C.A., Valle Junior, R.F., Varandas, S.G.P., Sanches Fernandes, L.F., Pacheco, F.A.L., 2016. The role of environmental land use conflicts in soil fertility: a study on the Uberaba River basin, Brazil. Sci. Total Environ. 562, 463–473.

Valle Junior, R.F., Varandas, S.G.P., Sanches Fernandes, L.F., Pacheco, F.A.L., 2014. Environmental land use conflicts: a threat to soil conservation. Land Use Policy 41, 172–185.

Veloz, S.D., 2009. Spatially auto-correlated sampling falsely inflates measures of accuracy for presence-only niche models. J. Biogeogr. 36 (12), 2290–2299.

Vladimir, V.N., Vapnik, V., 1995. The Nature of Statistical Learning Theory. Springer-Verlag New York (314 pp).

Woodward, D.E., 1999. Method to predict cropland ephemeral gully erosion. Catena 37 (3), 393–399.

Yesilnacar, E., Topal, T., 2005. Landslide susceptibility mapping: a comparison of logistic regression and neural networks methods in a medium scale study, Hendek region (Turkey). Eng. Geol. 79 (3), 251–266.

Youssef, A.M., Al-Kathery, M., Pradhan, B., 2015. Landslide susceptibility mapping at Al-Hasher area, Jizan (Saudi Arabia) using GIS-based frequency ratio and index of entropy models. Geosci. J. 19 (1), 113–134.

Zakerinejad, R., Märker, M., 2014. Prediction of Gully erosion susceptibilities using detailed terrain analysis and maximum entropy modeling: a case study in the Mazayejan Plain, Southwest Iran. Geogr. Fis. Din. Quat. 37 (1), 67–76.

Zakerinejad, R., Märker, M., 2015. An integrated assessment of soil erosion dynamics with special emphasis on gully erosion in the Mazayjan basin, southwestern Iran. Nat. Hazards 79 (1), 25–50.

Zare, M., Pourghasemi, H.R., Vafakhah, M., Pradhan, B., 2013. Landslide susceptibility mapping at Vaz Watershed (Iran) using an artificial neural network model: a comparison between multilayer perceptron (MLP) and radial basic function (RBF) algorithms. Arab. J. Geosci. 6 (8), 2873–2888.